AIP Journal of Applied Physics

# Ferroelectric properties in thin film barium titanate grown using pulsed laser deposition

Daniel J. R. Appleby, Nikhil K. Ponon, Kelvin S. K. Kwa, Srinivas Ganti, Ullrich Hannemann, Peter K. Petrov, Neil M. Alford, and Anthony O'Neill

Citation: Journal of Applied Physics **116**, 124105 (2014); doi: 10.1063/1.4895050
View online: http://dx.doi.org/10.1063/1.4895050
View Table of Contents: http://scitation.aip.org/content/aip/journal/jap/116/12?ver=pdfcov
Published by the AIP Publishing

**Articles you may be interested in**
The effect of stress on the dielectric and tunable properties of barium stannate titanate thin films
Appl. Phys. Lett. **94**, 052902 (2009); 10.1063/1.3073743

Orientation dependent ferroelectric properties in samarium doped bismuth titanate thin films grown by the pulsed-laser-ablation method
Appl. Phys. Lett. **89**, 032901 (2006); 10.1063/1.2221918

Effect of Li substitution on dielectric and ferroelectric properties of ZnO thin films grown by pulsed-laser ablation
J. Appl. Phys. **99**, 034105 (2006); 10.1063/1.2169508

Effects of poling, and implications for metastable phase behavior in barium strontium titanate thin film capacitors
Appl. Phys. Lett. **85**, 5010 (2004); 10.1063/1.1827934

Dielectric properties of pulsed laser deposited films of PbMg 1/3 Nb 2/3 –PbTiO 3 and PbSc 1/2 Nb 1/2 O 3 –PbTiO 3 relaxor ferroelectrics
J. Appl. Phys. **86**, 5179 (1999); 10.1063/1.371497

[This article is copyrighted as indicated in the article. Reuse of AIP content is subject to the terms at: http://scitation.aip.org/termsconditions. Downloaded to ] IP: 155.198.103.80 On: Tue, 11 Nov 2014 09:40:14

JOURNAL OF APPLIED PHYSICS 116, 124105 (2014)

# Ferroelectric properties in thin film barium titanate grown using pulsed laser deposition

Daniel J. R. Appleby,[1] Nikhil K. Ponon,[1] Kelvin S. K. Kwa,[1] Srinivas Ganti,[1] Ullrich Hannemann,[2] Peter K. Petrov,[2] Neil M. Alford,[2] and Anthony O'Neill[1]
[1]School of Electrical and Electronic Engineering, Newcastle University, Newcastle upon Tyne NE1 7RU, United Kingdom
[2]Department of Materials, Imperial College London, Royal School of Mines, Exhibition Road, London SW7 2AZ, United Kingdom

(Received 1 May 2014; accepted 8 August 2014; published online 24 September 2014)

The characteristics of polycrystalline $BaTiO_3$ metal-insulator-metal capacitors, fabricated using pulsed laser deposition, are investigated from room temperature to 420 K. The capacitance–voltage characteristics show ferroelectric behaviour at room temperature, with a phase transition to paraelectric at higher temperature. However, the permittivity response shows paraelectric behaviour across all measured temperatures. So $BaTiO_3$ exists here in a mixture of cubic and tetragonal phases. The $BaTiO_3$ films have a columnar structure, with grain size increasing with film thickness due to their increasing height but not diameter. This correlates with an increase in remnant polarization. The results support a size driven phase transition in thin films of polycrystalline $BaTiO_3$. © *2014 AIP Publishing LLC*. [http://dx.doi.org/10.1063/1.4895050]

## I. INTRODUCTION

Perovskite insulators have attracted particular attention for applications such as ferroelectric random access memories (FeRAM),[1] dynamic RAM,[2] and alternative gate materials for metal oxide semiconductor field effect transistors (MOSFETs).[3] A recent review details their short-term and future prospects for the nanoelectronics industry, further proof of the need to integrate this promising material in next generation devices.[4] A particular region of interest in these materials is the ferroelectric phase, which allows polarization to be retained in the absence of an applied electric field. Ferroelectricity has been the subject of numerous past studies,[5–8] and is of most relevance in non-volatile memory applications due to its ability to retain its charge state when power is removed. However, the ferroelectric phase is subject to varying degrees of intrinsic and/or extrinsic influences, ranging from elemental composition,[9] annealing, growth technique,[10] and straining,[11] among others.[12–16] Therefore, it is important to understand the quality of perovskites in terms of their demonstrated ferroelectric properties.

The phase of a perovskite is primarily dictated by temperature and described by the Curie-Weiss law, given by

$$\chi = \frac{C}{T - T_c}, \quad (1)$$

where $\chi$ is the dielectric susceptibility, T is the operating temperature, $T_c$ is the Curie temperature, and C the Curie constant. The phase of a perovskite will transition at a temperature $T = T_c$; however, in certain materials such as barium titanate ($BaTiO_3$, BTO), the phase transition temperature can be approximately 10 K above $T_c$.[17]

From Eq. (1), it follows that by increasing the operating temperature beyond $T_c$, the material will show decreasing susceptibility, and in turn permittivity ($\chi = \varepsilon_r - 1$, where $\varepsilon_r$ is the relative permittivity of the material). In contrast, operating below $T_c$ should give negative $\chi$, which leads to instability, and hysteretic characteristics ensue. The aforementioned properties are descriptive of the paraelectric phase when $T > T_c$, and the ferroelectric phase in cases when $T < T_c$. A key property of a perovskite material is its phase transition temperature, $T_c$. For the case of BTO in bulk or powder form, this temperature is approximately 393 K and where the permittivity is a maximum (Eq. (1)).[18] However, experimentally this property is known to change, particularly when dealing with thin film perovskites, and the permittivity peak tends to broaden or shift altogether.[19] In the high temperature phase ($T > T_c$), the perovskite crystal is cubic due to thermal agitation. Decreasing the operating temperature past the phase transition point ($T < T_c$) the perovskite crystal is tetragonal; long-range coulombic ordering results due to the balance of the thermal and electrostatic forces, allowing an elongation of the crystal c-axis and the creation of a built-in permanent dipole. The tetragonal deformation of a ferroelectric crystal allows alignment and subsequent reorientation of these permanent dipoles through the application of an external electric field.

A so-called "size driven phase transition" has been studied previously, specifically on particles[20] or freestanding films[22] of perovskite material. It places a critical limit on crystal grain size, such that a smaller grain structure shifts the phase transition temperature to lower values. Therefore, the size driven phase transition leads to materials that are paraelectric in phase at operating temperatures previously expected to be in the ferroelectric phase. Numerous studies on BTO nanoparticles have estimated a critical grain size, below which no ferroelectric properties are seen, to lie between 17 and 190 nm [Ref. 20 and references therein]. The grain size dependence has also been incorporated into Landau-Ginsburg-Devonshire theory in which grain size was varied from 50 to 1200 nm in dense BTO ceramics.[21] The results showed progressively lesser tetragonal phase with

 © 2014 AIP Publishing LLC

[This article is copyrighted as indicated in the article. Reuse of AIP content is subject to the terms at: http://scitation.aip.org/termsconditions. Downloaded to ] IP: 155.198.103.80 On: Tue, 11 Nov 2014 09:40:14

decreasing grain size, in concurrence with a shift in the phase transition temperature to lower values as the grain size reduces. Conversely, a grain size dependence on thin film $PbTiO_3$ was studied, which showed a transition from multi-domain to single domain structures at 150 nm grain size or less.[22] The retained tetragonal phase in the single domain structure exhibited a lack of polarization switching under the application of an electric field and low permittivity. The results are attributed to single domain structures in the smaller grains due to the inherent lack of domain walls and their subsequent movement. However, this result was measured on a free-standing film, and hence suffered no influence from the substrate.

In this study, thin films of BTO deposited by pulsed laser deposition (PLD) are investigated. The films are grown on Pt/Ti/$SiO_2$/Si substrates, and investigated in terms of ferroelectricity for Si integration applications. We show that thin films of BTO are in a mixed phase relationship, consisting of the cubic paraelectric phase, in addition to the tetragonal ferroelectric phase. Furthermore, it is shown that the cubic phase has a tendency to dominate at room temperature. The dominant cubic phase leads to a measured reduction in the overall remnant polarization, a common occurrence frequently reported in the literature[23,24] in terms of thin film and grain size dependence. The results confirm a size driven phase transition in thin films clamped to a substrate with columnar structures. The experiments indicate that increasing the heights of the columns by growing thicker films increases the remnant polarization in the thin films. The remnant polarization increase is due to an increase in grain size as the columns grow in height. With an increase in the film thickness, the column widths remain approximately 30 nm in size.

## II. EXPERIMENT

A BTO thin film of 160 nm thickness was deposited on a Pt/Ti/$SiO_2$/Si stack using PLD at a growth temperature of 740 °C. Further BTO films of 280 nm and 380 nm were also deposited for thickness dependence studies. The PLD system was equipped with a KrF excimer laser from Lambda Physik. Before deposition, the substrate was heated up to a deposition temperature of 740 °C. The deposition was performed at a repetition rate of 5 Hz in an oxygen pressure of 100 mTorr. The energy density of the focussed laser beam on the target was 4 J/$cm^2$. After deposition, the vacuum chamber was flooded with oxygen up to 500 Torr and the sample was cooled down to room temperature at a cooling rate of 10 °C/min. The Pt substrate layer (100 nm) and the Ti adhesion layer (10 nm) were deposited using electron beam evaporation. Pt top electrodes with diameters ranging from 50 to 300 $\mu$m were then fabricated to create metal-insulator-metal (MIM) structures, which were used for electrical measurements.

Small-signal capacitance-voltage (CV) electrical measurements were taken at temperatures ranging from room temperature (300 K) to 420 K. CV measurements were taken at 1 MHz and consisted of both forward (negative to positive sweep) and reverse (positive to negative sweep) biasing to analyse the BTO film. All remaining measurements were taken at room temperature. Large-signal hysteresis measurements were taken on a Radiant Precision Premier II. X-ray diffraction (XRD) spectra were acquired using Panalytical x'pert and the Raman spectra were acquired by a HORIBA scientific LabRam using a 514 nm laser. Electrostatic force microscopy (EFM) images were taken using an NSC 14 Au/Cr cantilever. Atomic force microscopy (AFM) in non-contact mode was also conducted to verify grain size using a non-contact high resonance frequency–reflex coating tip.

## III. RESULTS

### A. Electrical

Figure 1 shows the CV characteristics for a MIM capacitor with a BTO insulating layer of 160 nm thick performed at two different temperatures, 300 K and 420 K. Measurements performed at both temperatures should exhibit ferroelectric and paraelectric characteristics, respectively, since the phase transition temperature $T_c = 393$ K. At 300 K, measurements show two distinct curves, with the applied forward and reverse bias direction shown by the arrows. The curves indicate a two peak ("butterfly") trend in the measurement, and this is attributed to the polarization switching in a ferroelectric, i.e., the material displays directionally dependent characteristics with applied bias through its hysteretic polarization ($P \neq 0$ at $V = 0$). These results are indicative of ferroelectricity in BTO measured at 300 K.

The 160 nm thick BTO capacitor was measured at 420 K in order to induce a phase transition. The CV characteristics shift as the measurement temperature increases past the bulk value of $T_c$ (Fig. 1). The intermediate measurements (not shown) between temperatures 300 K and 420 K evolve gradually with increasing temperature towards the characteristics seen at 420 K. The double capacitance peaks observed at 300 K converge to a single peak and the butterfly trend is lost. The high temperature measurement is indicative that a phase transition has taken place in the BTO film such that each unit cell is now cubic and no longer retains any polarization.

Effective permittivity is determined for the 160 nm thick BTO capacitor using the parallel-plate capacitor relationship of the MIM structure. The permittivity response in a

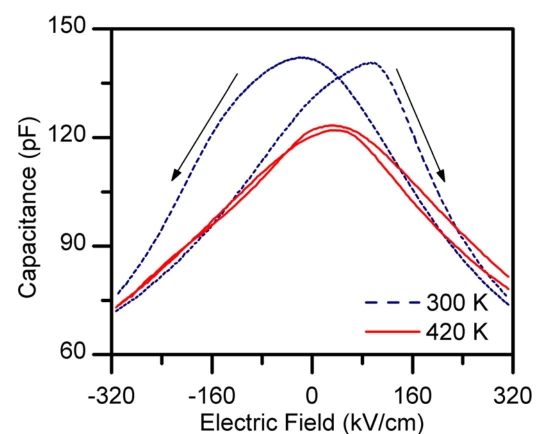


FIG. 1. Capacitance-voltage measured on the Pt/$BaTiO_3$ (160 nm)/Pt capacitor at 300 K and 420 K. Electric field is taken as $V/t_{ox}$, where $t_{ox}$ is the thickness of the $BaTiO_3$ film.

[This article is copyrighted as indicated in the article. Reuse of AIP content is subject to the terms at: http://scitation.aip.org/termsconditions. Downloaded to ] IP: 155.198.103.80 On: Tue, 11 Nov 2014 09:40:14

perovskite may show evidence of a phase transition in accordance with Eq. (1). When the ferroelectric transitions into the paraelectric phase, the permittivity will increase, reaching a maximum at the phase transition temperature, 393 K.[18] From the capacitance measurements shown in Fig. 1, it is expected that a peak permittivity will be seen at approximately 400 K. This would suggest a phase transition in the 160 nm thick BTO film.

Figure 2 shows the extracted effective permittivity variation with temperature from capacitance measurements using the parallel-plate relationship. Increasing the temperature towards 400 K, there is an absence of any peak in the permittivity. In contrast, measurements on freestanding BTO showed permittivity increasing sharply from approximately 380 K, and reaching a peak Curie anomaly at 400 K, demonstrating its ferroelectric nature.[19] Fig. 2 also shows that permittivity increases when the film thickness was increased from 160 nm to 280 nm. The permittivity further increases for the 380 nm thick BTO film. The trend shown here is indicating a paraelectric characteristic for all the three thicknesses where the permittivity is decreasing with increasing temperature, as described by Eq. (1). The result suggests that the phase transition has shifted to a lower temperature, whereby the paraelectric phase is induced at $T < T_c = 393$ K. However, the permittivity analysis contradicts the CV measurements in Fig. 1, which shows a convergence of the peak capacitance points when the temperature is increased to 420 K. Moreover, an increase in permittivity with increase in thickness points toward a change in the crystal structure of the BTO film with thickness.

The electrical results for the BTO capacitor disagree in terms of the properties displayed: the butterfly CV trend in Fig. 1 shows evidence for the tetragonal phase, while the permittivity response with temperature in Fig. 2 suggests a paraelectric phase based on Curie-Weiss law. The results lead to a conclusion that the film is in a mixed phase condition. The tetragonal part is responsible for the butterfly CV measurements, while the cubic phase dictates the permittivity response with temperature. The cubic phase is thought to be the dominating contribution due to the overriding paraelectric response to permittivity when the temperature increases. High concentrations of the cubic phase will manifest as minimal remnant polarization, which is apparent in a number of studies.[23] The measured permittivity is an effective permittivity, which has contributions from both cubic and tetragonal phase. An increase in effective permittivity with thickness can then be manifested as an increase in percentage of tetragonal phase with increase in thickness of the film. Frequency dependence on the capacitance was also measured for values ranging from 1 kHz to 1 MHz. The reduction in capacitance with increase in frequency was found to be negligible. A nearly constant capacitance for the measured frequency range points to a defect free film structure. Minimal remnant polarization in the BTO capacitors is investigated with large-signal hysteresis measurements in Sec. IV.

### B. Material

In order to investigate the material characteristics and mixed phase properties of the BTO film, EFM, XRD, and Raman spectra were taken at room temperature. Before the EFM images were taken, in order to polarize the BTO, −5 V was applied to the bottom Pt electrode and a 4 $\mu$m × 4 $\mu$m area was scanned in contact mode. The EFM images were taken across a 6 $\mu$m × 6 $\mu$m area which covers the previously polarized area. The alternating modulation applied to the tip had an amplitude of 0.8 V, and a frequency of 20 kHz.

XRD spectra (Fig. 3) of the 160 nm thick film is performed to investigate the crystallinity and to determine growth orientation. Results from the 280 and 380 nm thick BTO films are also shown and discussed in Sec. IV. The XRD peak intensity increased with increase in film thickness since the intensity is proportional to the volume of diffracting planes. From the results, it can be concluded that the BTO film is polycrystalline with random orientation, as evident from the numerous diffraction peaks in the spectrum. Therefore, the BTO film consists of randomly oriented grains with intersecting grain boundaries. Peak splitting in XRD spectra may show evidence for the tetragonal phase in a

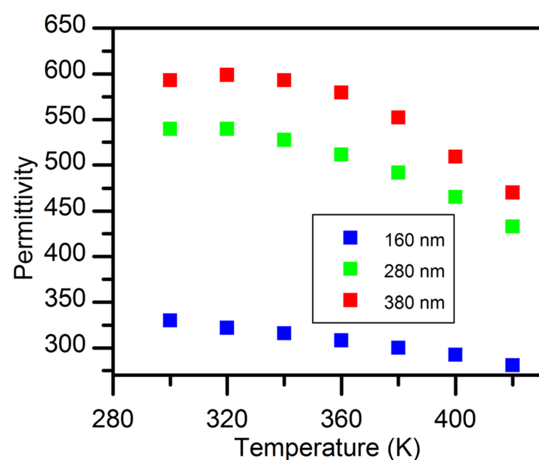


FIG. 2. Effective permittivity measured on the Pt/$BaTiO_3$/Pt capacitor as a function of increasing temperature. Permittivity is extracted from the parallel-plate capacitor relationship.

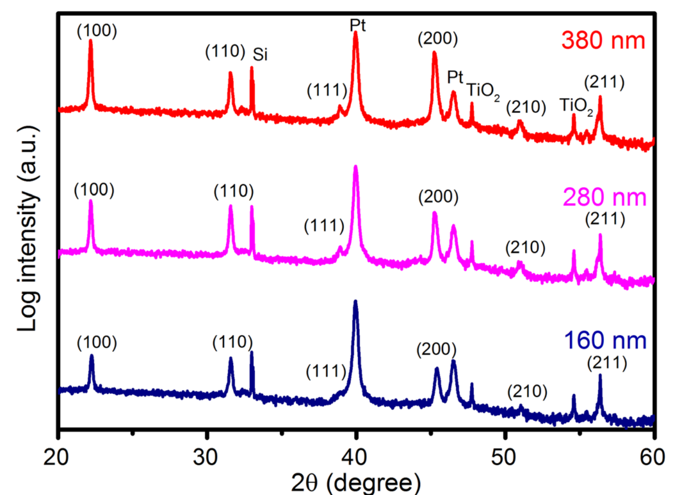


FIG. 3. XRD spectra of the BTO films with varying film thickness. Orientations of BTO are labelled with remaining contributions originating from Si, Pt, and Ti.

[This article is copyrighted as indicated in the article. Reuse of AIP content is subject to the terms at: http://scitation.aip.org/termsconditions. Downloaded to ] IP: 155.198.103.80 On: Tue, 11 Nov 2014 09:40:14

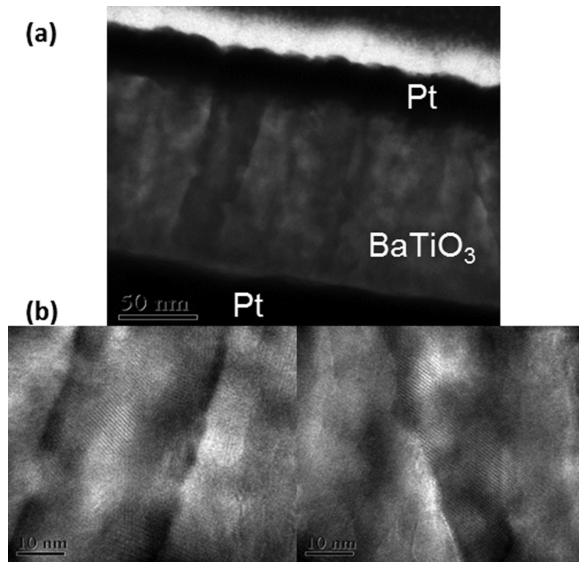


FIG. 4. TEM image of the 160 nm thick BTO sample. (a) Image shows the cross section of the full film thickness situated between the dark contrasting Pt electrodes. (b) Images show high resolution TEM highlighting individual columns.

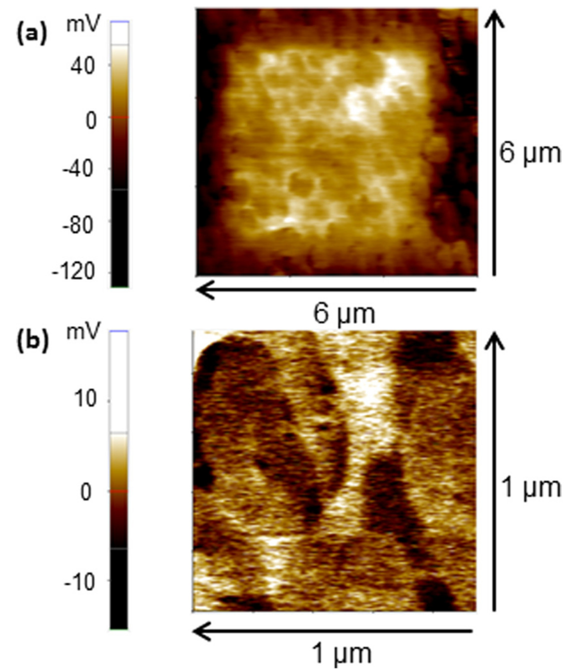


FIG. 5. EFM image of polycrystalline BTO at 160 nm thick (a). BTO is non-uniformly polarized. High resolution scan shows that it is a mixture of polarizable and non-polarizable domains (b).

perovskite crystal. The data presented in Fig. 3 does not signify any peak splitting; however, this is likely to be due to the resolution of the XRD measurement and as such the results do not factor into the conclusion about the phase of the BTO.

Further understanding of the structure of the BTO film can be gained through the TEM imaging in Fig. 4 for the 160 nm thick sample. The image in Fig. 4(a) shows the full BTO film thickness situated between the dark contrasting Pt electrodes. It is apparent that the film has grown in a columnar structure, originating from the initial bottom Pt electrode. Each column spans the full film thickness and they coalesce towards the top Pt electrode; therefore, each column height is the full thickness of the given film. From Fig. 4(a), each column width is estimated at 30 nm. Also shown in Fig. 4(b) are high resolution TEM images of the individual BTO columns. The results show that, taking into account the influence of Moiré fringes, each column is a uniform grain of single orientation, leading to grain boundaries at the column edges.

The EFM technique is applied to study any remnant polarization and domain structure in the BTO film. Fig. 5 shows the EFM scan of $6\,\mu m \times 6\,\mu m$ area on the surface of the 160 nm thick BTO film. The polarized $4\,\mu m \times 4\,\mu m$ region appears as a bright square, in sharp contrast with the outer un-polarized area. Colour variation in the polarized region as shown in Fig. 5 also indicates that the film is non-uniformly polarized. The result is further highlighted by a magnified scan of $1\,\mu m \times 1\,\mu m$ on the polarised area, clearly showing highly contrasted regions. The dark regions indicate non-polarizable domains, whereas white regions show the polarized domains. The cubic phase in BTO does not retain the spontaneous polarization upon the removal of an external field, whereas in the ferroelectric tetragonal phase it does. The co-existence of polarizable and non-polarizable domains confirms the presence of both cubic phase and tetragonal phase in polycrystalline BTO, in adherence with the previous results.

Raman spectra of thin film and bulk ceramic BTO from $100\,cm^{-1}$ to $800\,cm^{-1}$ at room temperature are given in Fig. 6. BTO reveals Raman active bands around 250, 306, 520, and $720\,cm^{-1}$. A sharp peak at approximately $300\,cm^{-1}$ and $720\,cm^{-1}$ is a characteristic of tetragonal BTO.[25] The

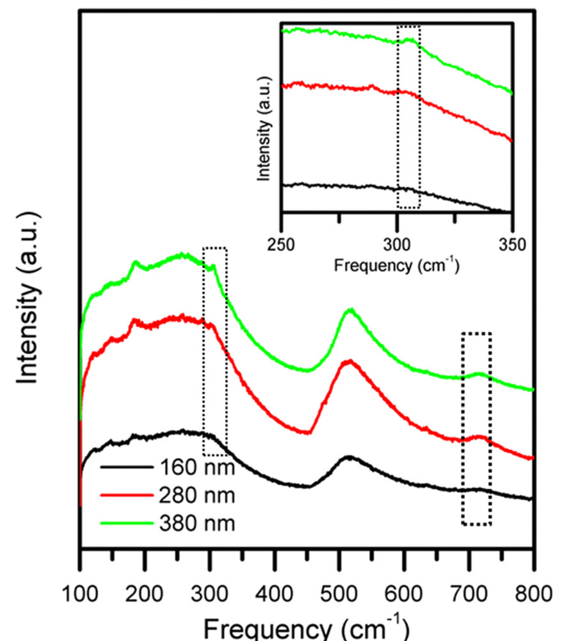


FIG. 6. Raman spectra of polycrystalline BTO as a function of increasing thickness. Dashed region shows BTO has a reduced peak intensity around $300\,cm^{-1}$ and $720\,cm^{-1}$ indicating presence of both cubic and tetragonal phases. Inset highlights that the peak intensity at $300\,cm^{-1}$ increases with increasing film thickness.

[This article is copyrighted as indicated in the article. Reuse of AIP content is subject to the terms at: http://scitation.aip.org/termsconditions. Downloaded to ] IP: 155.198.103.80 On: Tue, 11 Nov 2014 09:40:14

300 $cm^{-1}$ and 720 $cm^{-1}$ peak disappears as the phase changes from tetragonal to cubic, whereas the 250 and 520 $cm^{-1}$ peaks remain the same. Data for the 160 nm thick BTO film presented here show a reduced intensity peak around 300 $cm^{-1}$ and 720 $cm^{-1}$ compared to a bulk ceramic. The intensity of the Raman peaks is not affected by crystallographic orientation. Therefore, the reduction in the intensity of the Raman peak corresponding to the tetragonal phase (300 $cm^{-1}$) indicates the presence of both cubic and tetragonal phases, further supporting the results shown previously. Analysis of the Raman spectra of all BTO thicknesses studied here is given in Sec. IV.

## IV. DISCUSSION

Based on the previous results, thin film BTO is observed to be in a mixed phase condition comprising cubic and tetragonal parts. The butterfly CV trend and bright contrasting regions in EFM confirm the existence of the tetragonal phase. The permittivity response with temperature, dark contrasts in EFM, and lack of any Raman peak at 300 $cm^{-1}$ show evidence for the cubic phase. The studies discussed were for the 160 nm film thickness, which showed polycrystalline, randomly oriented grains in a columnar structure. The discussion will now turn to the thickness dependence of the films and 280 nm and 380 nm thick films will be compared with the results of the 160 nm thick film.

The remaining XRD spectra for the 280 nm and 380 nm thick films are presented in Fig. 3. The results are unchanged to those described previously for the 160 nm thick film. Each film thickness shows a polycrystalline and randomly oriented grain structure. Therefore, an increasing film thickness does not impact the texture or crystallinity of the BTO films.

The Raman spectra for the 280 nm and 380 nm thick films are studied, particularly the peak at 300 $cm^{-1}$ and 720 $cm^{-1}$ indicative of the tetragonal phase. Fig. 6 shows the full range of each spectrum, and the inset reflects the magnified region of the peak of interest. As the film thickness is increased, both the 300 $cm^{-1}$ and 720 $cm^{-1}$ peaks are seen to increase in intensity. These results mean that the contribution from the tetragonal phase increases as the thickness of the films increase. Consequently, an increasing film thickness should lead to an increase in remnant polarization.

Figure 7 shows a large-signal hysteresis measurement on the 380 nm thick sample. The inset in Fig. 7 also shows the remnant polarization measured in each sample to corroborate the thickness dependent Raman results discussed above. From the results, a clear thickness dependence is evident on the remnant polarization, which increases with BTO film thickness, leading to a confirmation of the Raman results. Therefore, it is initially inferred that an increase in the film thickness has increased the grain size of the film. In accordance with the size driven phase transition, the larger grains in the thicker films will be tetragonal and contribute to the increased remnant polarization. Thus, the concentration of the cubic phase in these mixed phase films will be reduced in thicker films.

In order to verify any changes in the grain structure of the films, AFM topography scans are conducted and shown in

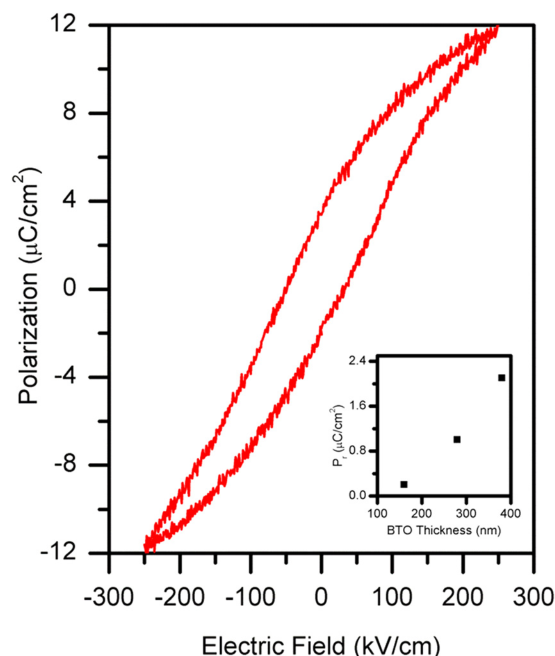


FIG. 7. Large signal hysteresis measurements of the 380 nm thick BTO film. Inset shows the measured remnant polarization as a function of film thickness.

Fig. 8. Each image shows an unchanged topography, which demonstrates an unchanging grain diameter as the film thickness is increased. However, from the TEM images of the 160 nm thick film in Fig. 4, BTO is known to grow in a columnar structure. Therefore, as the film thickness is increased the height of each individual column increases, while the diameter of each column stays constant as measured in the AFM scans. The increasing remnant polarization with film thickness is therefore due to an increase in the volume of each individual column as they grow in height. The increase in volume will favour the tetragonal phase whereby a larger number of dipoles are allowed to align along the polar axis, leading to the increase in remnant polarization. Ferroelectricity as a cooperative phenomenon favours an increase in the number of dipoles available for interaction, leading to an energetically stable ferroelectric phase. Previous studies discuss the number of required dipoles in terms of a correlation volume.[26] In the polycrystalline films with no preferred orientation, a similar effect should be seen if the diameter of the columns increases, which would be reflected in a changing topography in AFM scans. An increasing contribution from the ferroelectric phase (tetragonal phase) with thickness is also evident from the temperature dependent permittivity measurements. A large increase in permittivity with thickness is due to the percentage increase in tetragonal phase in the total volume.

## V. SUMMARY

Analysis of thin film BTO integrated with Si on Pt/Ti/$SiO_2$/Si substrates showed evidence of a mixed phase property in the films. The mixed phase film explains the low remnant polarization in thin film BTO as reported in the literature.[23] Large-signal measurements showed that

[This article is copyrighted as indicated in the article. Reuse of AIP content is subject to the terms at: http://scitation.aip.org/termsconditions. Downloaded to ] IP: 155.198.103.80 On: Tue, 11 Nov 2014 09:40:14

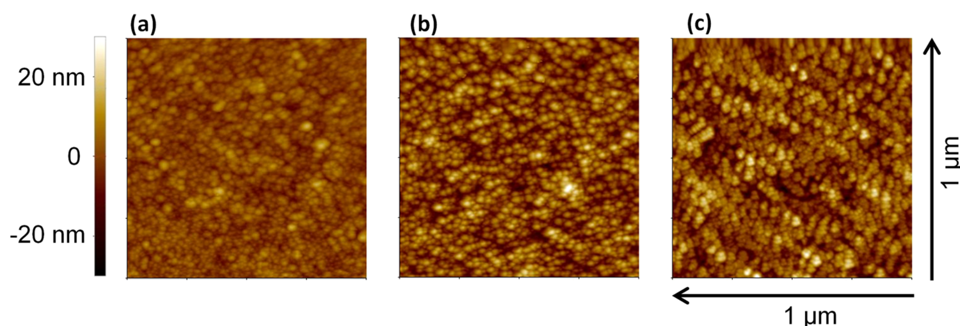


FIG. 8. AFM topography scans of the 160 nm (a), 280 nm (b), and 380 nm (c) thick films.

increasing the film thickness led to an increase in the remnant polarization. The Raman spectra also confirmed that an increase in the film thickness correlated with increasing peak intensities at 300 $cm^{-1}$, which is indicative of the tetragonal phase. XRD results showed that the crystallinity and texture stay constant with increasing film thickness. Furthermore, AFM and TEM imaging showed that the films grow in a columnar structure in which an individual column stays at a constant diameter as the film thickness increases. The results are such that as the films are grown at increasing thicknesses, the variable in terms of film structure is the increase in the height of each individual column.

The size driven phase transition sets a critical grain size in order for a material to display ferroelectric properties. In dense BTO ceramics, the tetragonal phase was shown to be progressively less prominent.[21] Here, we show that for a thin film BTO grown in a columnar structure, the height of the individual column acts to increase the remnant polarization due to the increasing contribution from the tetragonal phase. In each film, the diameter of the columns stays at an approximate 30 nm in size.

## ACKNOWLEDGMENTS

This work was supported by EPSRC and Intel Ireland.

[1]T. Mikolajick, C. Dehm, W. Hartner, I. Kasko, M. J. Kastner, N. Nagel, M. Moert, and C. Mazure, Microelectron. Reliab. **41**, 947 (2001).
[2]A. I. Kingon, J.-P. Maria, and S. K. Streiffer, Nature **406**, 1032 (2000).
[3]A. I. Khan, D. Bhowmik, P. Yu, S. J. Kim, X. Pan, R. Ramesh, and S. Salahuddin, Appl. Phys. Lett. **99**, 113501 (2011).
[4]J. F. Scott, Science **315**, 954 (2007).
[5]G. C. Danielson, Acta Crystallogr. **2**, 90 (1949).
[6]W. J. Merz, Phys. Rev. **91**, 513 (1953).
[7]V. G. Bhide, R. T. Gondhalekar, and S. N. Shringi, J. Appl. Phys. **36**, 3825 (1965).
[8]P. Wurfel and I. P. Batra, Phys. Rev. B **8**, 5126 (1973).
[9]B. A. Baumert, L.-H. Chang, A. T. Matsuda, T.-L. Tsai, C. J. Tracy, R. B. Gregory, P. L. Fejes, N. G. Cave, W. Chen, D. J. Taylor, T. Otsuki, E. Fujii, S. Hayashi, and K. Suu, J. Appl. Phys. **82**, 2558 (1997).
[10]Y. Sakabe, Y. Yamashita, and H. Yamamoto, J. Eur. Ceram. Soc. **25**, 2739 (2005).
[11]H. W. Jang, A. Kumar, S. Denev, M. D. Biegalski, P. Maksymovych, C. W. Bark, C. T. Nelson, C. M. Folkman, S. H. Baek, N. Balke, C. M. Brooks, D. A. Tenne, D. G. Schlom, L. Q. Chen, X. Q. Pan, S. V. Kalinin, V. Gopalan, and C. B. Eom, Phys. Rev. Lett. **104**, 197601 (2010).
[12]N. A. Pertsev, A. G. Zembilgotov, and A. K. Tagantsev, Phys. Rev. Lett. **80**, 1988 (1998).
[13]J. Junquera and P. Ghosez, Nature **422**, 506 (2003).
[14]D. D. Fong, G. B. Stephenson, S. K. Streiffer, J. A. Eastman, O. Auciello, P. H. Fuoss, and C. Thompson, Science **304**, 1650 (2004).
[15]S. Tong, B. Ma, M. Narayanan, S. Liu, U. Balachandran, and D. Shi, Mater. Lett. **106**, 405 (2013).
[16]Q. Yu, J.-F. Li, W. Sun, Z. Zhou, Y. Xu, Z.-K. Xie, F.-P. Lai, and Q.-M. Wang, J. Appl. Phys. **113**, 024101 (2013).
[17]S. Kwon, W. Hackenberger, E. Alberta, E. Furman, and M. Lanagan, IEEE Electr. Insul. Mag. **27**, 43 (2011).
[18]G. H. Jonker and J. H. Van Santen, Science **109**, 632 (1949).
[19]M. M. Saad, P. Baxter, R. M. Bowman, J. M. Gregg, F. D. Morrison, and J. F. Scott, J. Phys.: Condens. Matter **16**, L451 (2004).
[20]K. Suzuki and K. Kijima, J. Mater. Sci. Lett. **40**, 1289 (2005).
[21]Z. Zhao, V. Buscaglia, M. Viviani, M. T. Buscaglia, L. Mitoseriu, A. Testino, M. Nygren, M. Johnsson, and P. Nanni, Phys. Rev. B **70**, 024107 (2004).
[22]S. B. Ren, C. J. Lu, J. S. Liu, H. M. Shen, and Y. N. Wang, Phys. Rev. B **54**, R14337 (1996).
[23]L. Huang, Z. Chen, J. D. Wilson, S. Banerjee, R. D. Robinson, I. P. Herman, R. Laibowitz, and S. O'Brien, J. Appl. Phys. **100**, 034316 (2006).
[24]R. Flores-Ramirez, A. Huanosta, E. Amano, R. Valenzuela, and A. R. West, Ferroelectrics **99**, 195 (1989).
[25]Y. Shiratori, C. Pithan, J. Dornseiffer, and R. Waser, J. Raman Spectrosc. **38**, 1288 (2007).
[26]*Physics of Ferroelectrics: A Modern Perspective, Topics in Applied Physics*, edited by K. Rabe, C. H. Ahn, and J.-M. Triscone (Springer, Berlin, 2007), Vol. 105.

[This article is copyrighted as indicated in the article. Reuse of AIP content is subject to the terms at: http://scitation.aip.org/termsconditions. Downloaded to ] IP: 155.198.103.80 On: Tue, 11 Nov 2014 09:40:14